

## APPROACH OF NONLINEAR CONTROL APPLIED ON PVTOL WITH CARTESIAN DYNAMIC RESTRICTED

**Omar Sanchez-Rodriguez**

CIC  
Instituto Politecnico Nacional  
Mexico  
osanchezrod@gmail.com

**Ricardo Barron-Fernandez**

CIC  
Instituto Politecnico Nacional  
Mexico  
barron2131@gmail.com

**Juan Carlos Chimal-Eguia**

CIC  
Instituto Politecnico Nacional  
Mexico  
chimale@cic.ipn.mx

### Abstract

This work is directed toward stabilizing a PVTOL by two rotors with restricted spatial mobility. The problem of controlling the system is solved using a new method proposed by Astolfi and Ortega, named Immersion and Invariance stabilization. The method consists of a controller which is strengthened by immersion in a system with better performance characteristics and its invariance ensures that will converge to a point of stability. This is validated by numerical software simulation and implemented on a virtual reality environment which was designed in CAD software.

### Key words

Stabilizing, Controlling, Immersion and Invariance, PVTOL

### 1 Introduction

In recent years several studies have been generated concerning to the development of unmanned aerial vehicles more efficient, with better performance and higher yields, due to the need of aerospace vehicles to have small size and wide range of applications ranging from vehicular traffic monitoring, inspection of hazardous areas, border surveillance, weather measurement, search and rescue and disaster monitoring applications such as military in war zones where it is necessary to survey the area without risking the lives of pilots. One of the main objectives for researchers now is to achieve automated flight dynamics of such aircraft so as to be stable and perform in the neighborhood of a desired trajectory.

The problem addressed in this paper is to stabilize the decoupling between the longitudinal and lateral dynamics the study is then made on a dynamic PVTOL with cartesian restricted conditions, the system is described as a system with two propellers arranged at a distance above the longitudinal plane ( $x$ ) and translational dynamics restricted.

For this system we obtain a mathematical model

describing the dynamics of a rod actuated by two rotors for which we design a control algorithm that stabilizes the system, such algorithms are validated through software simulations and implementation in a Virtual reality environment. The paper is organized as follows, section 1 is a brief introduction and discusses the background, section 2 gives the mathematical model to study and analyze their properties, while in section 3 presents the control algorithm, sections 5 and 6 show the simulations and section 7 are the conclusions of the article.

During the last decade have been taking efforts by the scientific and technological community oriented stabilization and trajectory tracking of rotary wing aircraft.[Altug, Ostrowski and Taylor, 2005] propose a control algorithm to stabilize the cuatrorotor using artificial vision and a camera as the main sensor. They study two methods, used in the first control algorithm. Their results were successful tested in simulations.

In its paper [Heredia, Ollero, Bejar and Mahtani, (2008)] they deal with the problem of controlling an autonomous helicopter and do so by computer simulations of control strategies based on fuzzy logic and non-linear tracking control of two possible scenarios vertical ascent and simultaneous longitudinal and lateral movement. The controller consists of a MIMO (multiple inputs multiple outputs) inner loop for stabilization and four ties led to SISO in speed and position.

In its paper [Pounds, et al, 2006] conceived and developed a control algorithm for a four-rotor prototype they use inertial measurement unit (IMU for his syllables in English) for measuring the angular velocity and acceleration, using the linearization technique they conceive a dynamic model control. The results were tested by simulation.

[Vissiere and Petit, 2008] consider the problem of developing a modular system for real-time embedded control applications in UAVs, their efforts lead them toward programming and they propose the control strategies. To test its reported results implementing an ex-

tended Kalman filter at  $75Hz$  used for estimating the states of a small helicopter.

They [Chowdhary and Lorenz, (2005)] conceive stabilization of a VTOL UAV by considering the feedback states into line as a simple linear control technique with the only problem of the flight envelope. The problem is often accentuated due to improper linear model, the measurement noise in the sensors and external shocks. They present a control architecture based on a valid extension of the linear optimal control law for entire feedback states. An extended Kalman filter is used in the problem state and parameter estimation. Based on the estimation of the parameters feedback state gain is calculated by solving the Riccati equation for quadratic optimization control online.

In his doctoral thesis [Arda, (2006)] addresses the problem of designing an embedded system for a vehicle equipped with air cuatrirotor inertial sensors, the control system is developed in Matlab/Simulink and implemented in real time using Simulink module Real Time Windows Target. Then designs a linear quadratic regulator for stabilization of the attitude flight. The hardware it integrates a data acquisition card, DC drives, a set of sensors, DC motors and Draganflyer V Ti platform. Now [Salazar-Cruz, Escareno, Lara and Lozano (2007)] describes the design of an embedded control system for an unmanned aerial vehicle (UAV) capabilities cuatrirotor rate for stationary flights. The vehicle dynamic model is presented using Euler-Lagrange and propose a control strategy based on integer saturation, embedded control system architecture describes stationary autonomous flight. The main system components are a microcontroller, an inertial measurement unit (IMU), a global positioning system (GPS), and infrared sensors. Euler angles are calculated using a data fusion algorithm. Experimental results show that the control system works for indoor flying autonomous vehicles.

[Adigbil, (2007)] presents the development of a reliable remote control to assist in a mini air robot with four rotors and capabilities to ensure a stable flight. As a first phase dynamic model obtained by Euler-Lagrange equations and test three different types of control laws for feedback states, and sliding mode backstepping for stabilization and all UAV position, the author mentions that all of them were compared in simulations but not describe the advantages of each.

[Mian and Wang, (2008)] proposed a nonlinear controller for stabilizing a helicopter, the strategy is based on the saturation of integrators. Due to the positive achievements that have this type of strategy it was allowed to take into account the coupling conditions. The controller simulations showed good results in respect of other drivers, and thanks to embedded sensors and control is that it is capable of autonomous flight in real time. Their results show that the control strategy is able to perform tasks autonomously as take-off, landing and hovering.

Finally [Ollero and Merino, (2004)] discusses meth-

ods and technologies that have been applied in aerial robotics, several UAVs, summarizes the control techniques including control architectures and control methods.

## 2 Mathematical model

### 2.1 dynamic model

To obtain the dynamic model consider that the two rotors producing a force normal to the horizontal plane of the system. Because the system has two rotors that

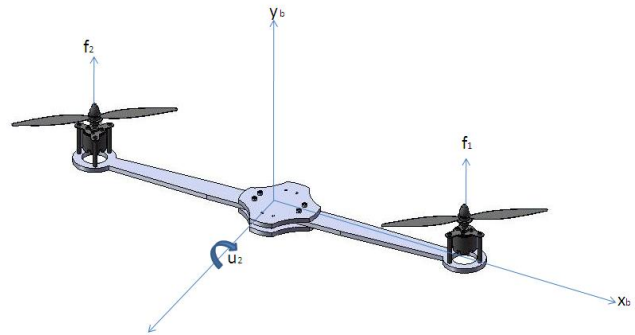


Figure 1. System model

provide the thrust force, the total thrust is given by,  $T_t = \sum_{i=1}^2 T_i$  the forces caused by the action of the motors  $T_1$  and  $T_2$  produce a torque about the center of gravity. The total rotational torque given by the following expression  $u_\theta = (T_2 - T_1)l$ , where  $l$  is the distance from the center of gravity of the system to the engine axis.

Realizing the analysis of forces, applying Newton's second law and considered as state variables to the energy accumulating elements which in this case is a mass that rotates at a speed about its center of gravity, the equation which models the dynamic behavior of the system is the following differential equation

$$J\ddot{\theta} + B\dot{\theta} = u \quad (1)$$

where  $\phi(u)$  is an unknown control function that depends on time

$$J\ddot{\theta} + B\dot{\theta} = \phi(u) \quad (2)$$

We spent to representation in first-order equations

$$\dot{\theta}_1 = \theta_2 \quad (3)$$

$$\dot{\theta}_2 = -\frac{B}{J}(\theta_2) + \frac{1}{J}\phi(u) \quad (4)$$

The model is represented in state variables, which are defined for the following states  $x_1 = \theta_1, x_2 = \theta_2$  and we obtain the following matrix representation

$$\dot{x} = f(x, u) = \begin{bmatrix} 0 & 1 \\ 0 & -\frac{B}{J} \end{bmatrix} x + \begin{bmatrix} 0 \\ \frac{1}{J} \end{bmatrix} [u] \quad (5)$$

The  $J$  value was obtained from an analysis of the model made in SolidWorks and  $B$  is the damping of the system modeled by the equation

$$B = -F | \dot{\theta} | \dot{\theta}$$

We analyze the stability of the system by calculating the characteristic polynomial of the open loop system which is

$$\lambda^2 + \lambda \frac{B}{J} \quad (6)$$

Besides we obtain the system eigenvalues  $\lambda_1 = 0$  and  $\lambda_2 = -\frac{B}{J}$ . So for any value of this system will have a zero eigenvalue and the other negative, we can only inferred internal stability, since the matrix  $A$  is not Hurwitz.

### 3 Control Algorithm Design

The control algorithm used to stabilize the bar system is based on the method proposed by [Astolfi and Ortega, (2003)], in the work we use asymptotic stabilization for design adaptive control laws of non-linear systems.

Consider a system of the form

$$\dot{x} = f(x, u)$$

and the basic problem it is to find a stabilizing control law  $u = u(x)$  (ie when it is possible) so that the closed loop system be either locally (globally) asymptotically stable. The proposed procedure for solving this problem consists of two steps. First find a target dynamic system  $\dot{\xi} = \alpha(\xi)$  to be locally (globally) asymptotically stable dimension strictly less than  $x$ , a mapping  $x = \pi(\xi)$ , and a function  $c(x)$ , such that

$$f(\pi(x), c(\pi(\xi))) = \frac{\partial \pi}{\partial \xi}(\xi) \alpha(\xi)$$

that is any trajectory  $x(t)$  of the system  $\dot{x} = f(x, c(x))$  is the image by mapping  $\pi(\cdot)$  of a path in the target system. Note that the mapping  $\pi : \xi \rightarrow x$  is an immersion, i.e. the range of  $\pi$  is equal to the dimension of  $\xi$ . Second, implement a control law that contributes to the attract variety  $x = \pi(\xi)$  and maintains closed loop

trajectories bounded. Thus it follows that the closed-loop system asymptotically behave as desired objective system and stability is ensured.

We resume the equations 3 and 4 and we rewrite

$$\dot{\theta}_1 = \theta_2 \quad (7)$$

$$\dot{\theta}_2 = \xi(t) + \frac{1}{J} \phi(u) \quad (8)$$

where  $\xi(t)$  is an unknown function that depends on time, and we get the following system

$$\dot{\theta}_1 = \theta_2 \quad (9)$$

$$\dot{\theta}_2 = \xi(t) + \frac{1}{J} u \quad (10)$$

Consider the following full-order target system, a new controller is designed for this system, where  $u = u(t)$  is any stabilizing control law for the system by feedback

$$z_1 = \theta_2 - \hat{\theta}_2 + \beta_1(\theta_1) \quad (11)$$

$$z_2 = \xi(t) - \rho_1 + \beta_2(\theta_1) \quad (12)$$

$$z_3 = \dot{\xi}(t) - \rho_2 + \beta_3(\theta_1) \quad (13)$$

to obtain the state variables of interest for immersion in the higher-order system, you must find a function  $\psi(x, z)$  that preserves the trajectories bounded and asymptotically stable zero dynamics

$$\theta_2 = z_1 + \hat{\theta}_2 - \beta_1(\theta_1) \quad (14)$$

$$\xi(t) = z_2 + \rho_1 - \beta_2(\theta_1) \quad (15)$$

$$\dot{\xi}(t) = z_3 + \rho_2 - \beta_3(\theta_1) \quad (16)$$

Suppose  $\ddot{\xi} \approx 0$ , and apply the following control input

$$u = J[(\rho_1 - \beta_2) + k_p \theta_1 + k_d \theta_2]$$

and replaced the equations 9 and 10 obtained for the following system

$$\dot{\theta}_1 = \theta_2 \quad (17)$$

$$\dot{\theta}_2 = -\xi + \rho_1 - \beta_2 + k_p \theta_1 + k_d \theta_2 \quad (18)$$

Consider that equation 12 is rewritten as follows

$$\dot{\theta}_1 = \theta_2 \quad (19)$$

$$\dot{\theta}_2 = -z_2 + k_p \theta_1 + k_d \theta_2 \quad (20)$$

and is derived from the target system for the function

that us to preserve the condition of stability

$$\dot{z}_1 = \xi + \frac{1}{J}u - \dot{\hat{\theta}}_2 + \frac{\partial\beta_1}{\partial\theta_1}\theta_2 \quad (21)$$

$$\dot{z}_2 = \dot{\xi} - \dot{\rho}_1 + \frac{\partial\beta_2}{\partial\theta_1}\theta_2 \quad (22)$$

$$\dot{z}_3 = -\dot{\rho}_2 + \frac{\partial\beta_3}{\partial\theta_1}\theta_2 \quad (23)$$

substitution is  $\xi$ ,  $\dot{\xi}$  and  $\theta_2$  in the above equations yield the following system

$$\begin{aligned} \dot{z}_1 = & z_2 + \rho_1 - \beta_2 + \frac{1}{J}u - \dot{\hat{\theta}}_2 \\ & + \frac{\partial\beta_1}{\partial\theta_1}(z_1 + \hat{\theta}_2 - \beta_1) \end{aligned} \quad (24)$$

$$\begin{aligned} \dot{z}_2 = & z_3 + \rho_2 - \beta_3 - \dot{\rho}_1 \\ & + \frac{\partial\beta_2}{\partial\theta_1}(z_1 + \hat{\theta}_2 - \beta_1) \end{aligned} \quad (25)$$

$$\dot{z}_3 = -\dot{\rho}_2 + \frac{\partial\beta_3}{\partial\theta_1}(z_1 + \hat{\theta}_2 - \beta_1) \quad (26)$$

are cleared again the variables of interest, leaving the following system

$$\dot{\hat{\theta}}_2 = \rho_1 - \beta_2 + \frac{1}{J}u + \frac{\partial\beta_1}{\partial\theta_1}(\hat{\theta}_2 - \beta_1) \quad (27)$$

$$\dot{\rho}_1 = \rho_2 - \beta_3 + \frac{\partial\beta_2}{\partial\theta_1}(\hat{\theta}_2 - \beta_1) \quad (28)$$

$$\dot{\rho}_2 = \frac{\partial\beta_3}{\partial\theta_1}(\hat{\theta}_2 - \beta_1) \quad (29)$$

This system complies with the condition of the  $\psi(\theta, z)$  preserve bounded the trajectories and stabilize at zero asymptotically. Now solve the problem of finding a function and a control  $u$  such that describe the invariant manifold . This requires the solution of a partial differential equation, this will start building considering the following system of equations, taken 21, 22 and 23 and replacing them  $z_1$ ,  $z_2$  and  $z_3$ , the system is

$$\dot{z}_1 = \frac{\partial\beta_1}{\partial\theta_1}z_1 + z_2 \quad (30)$$

$$\dot{z}_2 = \frac{\partial\beta_2}{\partial\theta_1}z_1 + z_3 \quad (31)$$

$$\dot{z}_3 = \frac{\partial\beta_3}{\partial\theta_1}z_1 \quad (32)$$

derives 30 and replaced 31

$$\dot{z}_1 = \frac{\partial\beta_1}{\partial\theta_1}z_1 + \dot{z}_2 = \frac{\partial\beta_1}{\partial\theta_1}z_1 + \frac{\partial\beta_2}{\partial\theta_1}z_1 + z_3 \quad (33)$$

derives 33 and replaced 32 and obtain

$$\dot{z}_1 = \frac{\partial\beta_1}{\partial\theta_1}z_1 + \frac{\partial\beta_2}{\partial\theta_1}z_1 + \dot{z}_3 = \frac{\partial\beta_1}{\partial\theta_1}z_1 + \frac{\partial\beta_2}{\partial\theta_1}z_1 + \frac{\partial\beta_3}{\partial\theta_1}z_1 \quad (34)$$

equals zero ref eq: obs25 and finally obtains a polynomial with terms that are partial differential equations

$$z_1^{(3)} + \beta_1\dot{z}_1 + \beta_2\dot{z}_1 + \beta_3z_1 = 0 \quad (35)$$

The final result is the system and the controller, where the variables of the controller are obtained from the equations 27, 28 and 29. The asymptotically stable system is described by the following equations

$$\dot{\theta}_1 = \theta_2 \quad (36)$$

$$\dot{\theta}_2 = -\frac{F}{J} + \frac{1}{J}u \quad (37)$$

$$u = J[(\rho_1 - \beta_2) + k_p\theta_1 + k_d(\hat{\theta}_2 - \beta_1)] \quad (38)$$

## 4 Results

### 4.1 Tuning to the controller gains and of the observer

In this section we validate the control algorithm through numerical simulation, the above results were done in *Matlab* and *Simulink*.

We make a first set of simulations in order to observe the behavior of both the observer gains and PD the controller gains. Figure 2 makes a first visualization of the behavior with different gains for the controller while the observer remains constant at 1.0, it is clear that the optimal gain is over 100 and under 1000. Therefore values are plotted in that interval, the figure 3 show the behavior to different values, it is easy to conclude that higher values show the negative overshoot the system is smaller, but the figure 2 shows that if the system is large does not stabilize at zero. Therefore be used for controller gain of 400.

As shown in figure 4 the constant controller gains are 1.0 and were varied observer gains. It is easy to see that the optimal gain is 1.35.

### 4.2 First simulation of the closed loop system

A first simulation of controller parameters and observer are showed in table 1

Polos del controlador	Polos del observador
1.0	1.0
1.0	1.0
1.0	

Table 1. System parameters for the first simulation

The figures 5 and 6 shows the position and the rotational speed of the closed-loop system. It is noticeable that both stabilize after a series of oscillations. Looking at figure 7, we can notice that the variable  $\hat{\theta}_2$  is

estimated and shows a similar behavior to the variable  $\theta_2$ , the figure 8 shows a comparison between the two variables, we observe that the observer estimates the variable  $\theta_2$  in 4.5 seconds. The figure 9 shows the estimation error of the observer and the figure 10 shows the control signal which stabilizes the system at zero degrees.

### 4.3 Second simulation of the closed loop system

This section gives a second simulation taking into account the poles obtained from the tuning gains. The parameters used for this simulation are from table 2

Polos del controlador	Polos del observador
400.0	1.35
400.0	1.35
400.0	

Table 2. System parameters for the second simulation

The figures 11 and 12 shows the position and the rotational speed of the closed-loop system, it can be noted that the stabilization is immediate. If we look at figure 13, we note that the variable estimated  $\hat{\theta}_2$ , shows a behavior equal to the variable  $\theta_2$ , figure 14 shows a comparison between the two variables, we observe that the observer estimates the variable  $\theta_2$  immediately. Figure 15 shows the estimation error of the observer and figure 16 shows the control signal which stabilizes the system at zero degrees. We can conclude that to properly tune the observer it shows excellent performance, as it stabilizes the system immediately, should also be noted that the dynamic quickest driver is having a significant impact on the performance of the control loop and the dynamics the observer must be just a little faster because otherwise the system becomes unstable, this due to saturation in the control loop.

The results of the simulation in virtual reality environment of the system are described satisfactory stabilization trajectories shown in graphs 5 and 11 unlike shown in a model 3D system. The figure 17 shows a stage of stabilization of the system and figure 18 show the stabilized system.

## 5 Conclusions

In this paper develops a control algorithm for a system consisting of a rod actuated by two rotors, the proposed algorithm is based on the theory proposed by Astolfi and Ortega [Astolfi and Ortega, (2003)]. This controller showed an excellent performance in the simulations when the gains were appropriate. In the simulations presented shows that the controller gain is the one

with greater presence in the system dynamics, however, a good choice of observer gains ensures a dynamic fast enough for the correct estimation of the state  $\theta_2$ , but caution is needed because a too rapid dynamics saturates the loop and leads to instabilities. The initial conditions are not important result in the stabilization of the system when stored below 45 degrees above the horizontal.

Graphs 9 and 15 show the estimation error, which can be verified as tends to be zero, again proper tuning makes gains error dynamics faster. The virtual reality model ahead helped visualize the behavior of the physical system. This facilitates the interpretation of the control algorithm and performance.

## 6 Acknowledgements

This work was done with support from CONACYT Mexico, COFAA IPN, EDI IPN, also work is associated with the projects SIP-20131599 y SIP-20131210. And is also associated with project SENER HIDRO-CARBUIROS 146515.

## References

- Adigbil, P. (2007). Nonlinear attitude and position control of a micro quadrotor using Sliding Mode and Backstepping Techniques. In *3rd US-European Competition and Workshop on Micro Air Vehicle Systems (MAV07) and European Micro Air Vehicle Conference and Flight Competition (EMAV2007)* Europe, 2007. pp. notavailable.
- Altug, E., Ostrowski, J.P. and Taylor, C.J. (2005) Control of a quadrotor helicopter using dual camera visual feedback. *The International Journal of Robotics Research*, **25/5**, pp. 329–341.
- Astolfi, A., Ortega, R. (2003) Immersion and Invariance: A new tool for Stabilization and Adaptive Control of Nonlinear Systems. *IEEE Transactions on Automatic Control*, **48**, pp. 590–606.
- Arda, K. (2006). *Design of control systems for a quadrotor flight vehicle equipped with inertial sensors*. Tesis doctoral de la Universidad de Atilim. Turquia.
- Bishop, R.H., Dorf, R.C. (2005). *Sistemas de Control Moderno*. Pearson. USA.
- Chi-Tsong, C. (1970). *Introduction to linear systems*. Rinehart and Winston line. New York USA
- Chi-Tsong, C. (1999). *Linear System Theory and Design*. Oxford University Press. New York, USA.
- Chowdhary, G. and Lorenz, S. (2005). Control of a VTOL UAV via Online Parameter Estimation. In *Guidance, Navigation, and Control Conference and Exhibit*.
- Close, C. and Frederick, D. *Modeling and Analysis of Dynamic Systems*. Jonh Wiley Sons Inc. USA.
- Dominguez, S., et all. *Control en el espacio de estados*. Prentice Hall. Madrid, Espaa.
- Heredia, G., Ollero, A., Bejar, M. and Mahtani, R. (2008). Sensor and actuator fault detection in small

autonomous helicopters. *Journal of IFAC of Mecha- tronics The Science of Intelligent Machines.*, **18**, pp. 90–99.

Hinrichsen, D. and Pritchard, A. *Mathematical Systems Theory Modeling State Space Analysis Stability and Robustness*. Springer. Germany.

Khalil, H. *Non linear systems*. Prentice Hall. USA.

Lozano, R. and et al. Real-time stabilization and tracking of a four mini rotorcraft. *IEEE Transactions on Control Systems Technology.*, **12**, pp. 510–516.

Mian, A.A. and Wang, D. (2008) Dynamic modelling and nonlinear control strategy for an underactuated quad rotor rotorcraft. *Journal of Zhejiang University*, pp. 539–545.

Ollero, A. and Merino, L. (2004) Control and percep- tion techniques for aerial robotics. *Annual Reviews in Control*, **28**, pp. 167–178.

Pounds, and et al.(2006). Nonlinear control for sys- tems with bounded inputs: Real-time embedded control applied to UAVs. In *IEEE Proceedings of the 45th Conference on Decision and Control* San Diego Cal- ifornia, E.U.A, 2006. pp. 5888–5893.

Salazar-Cruz, S., Escareno, J., Lara, D. and Lozano, R.(2007) Embedded control system for a four-rotor UAV. *International Journal of Adaptive Control and Signal Processing*, **21**, pp. 189–205.

Vissire, D. and Petit, N. (2008). An embedded sys- tem for small-scaled autonomous vehicles. In *Inter- national Conference on Informatics in Control, Au- tomation and Robotics*. pp. 158–164.

*Virtual Reality Toolbox 3.0 Help*

## Appendix A Graphics

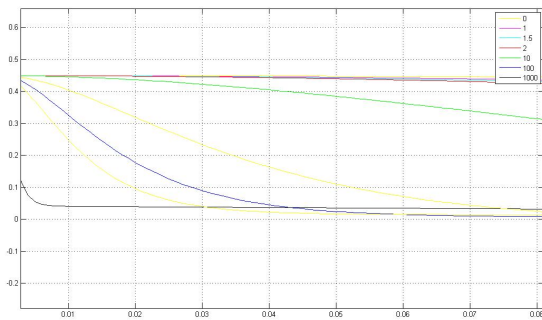


Figure 2. Observer gains

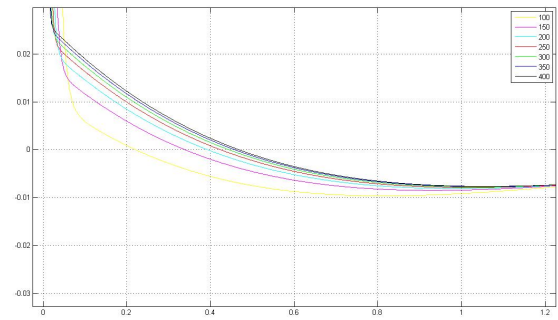


Figure 3. Controller gains in the 100 to 400 interval

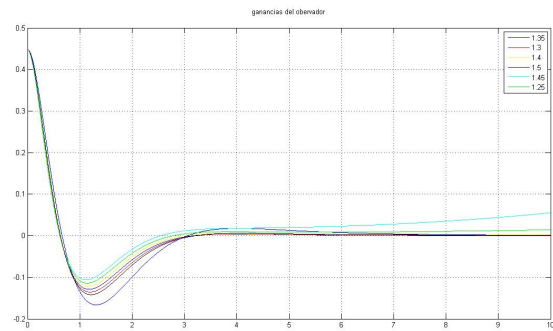


Figure 4. Observer gains in the 1.0 to 1.5 interval

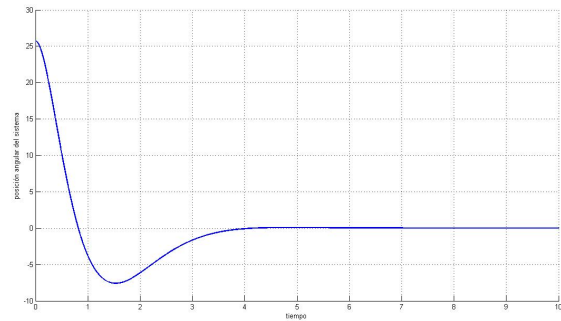


Figure 5. Closed loop system angular position  $\theta_1$

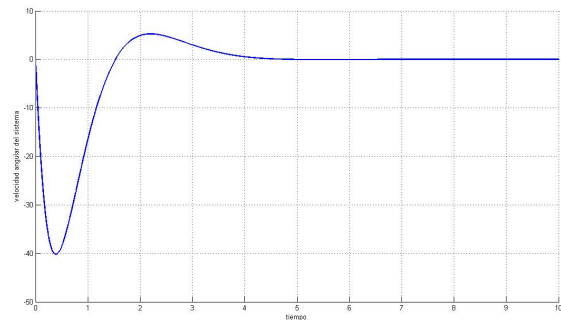


Figure 6. Closed loop system angular velocity  $\theta_2$

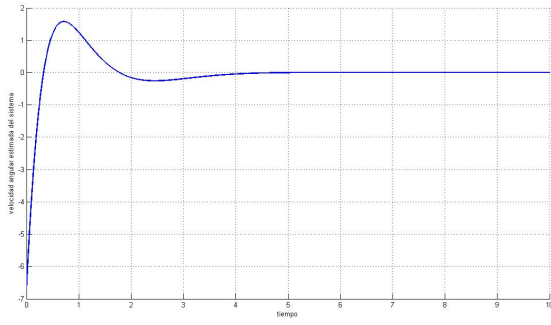


Figure 7. Closed loop system estimated angular velocity  $\hat{\theta}_2$

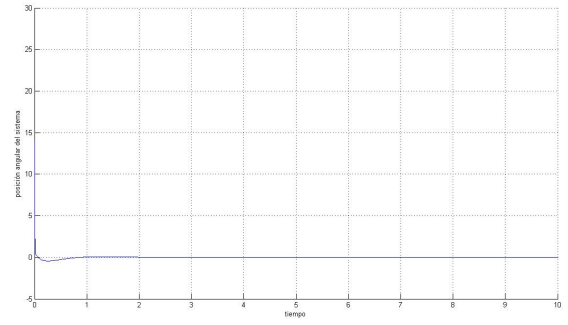


Figure 11. Closed loop system angular position  $\theta_1$

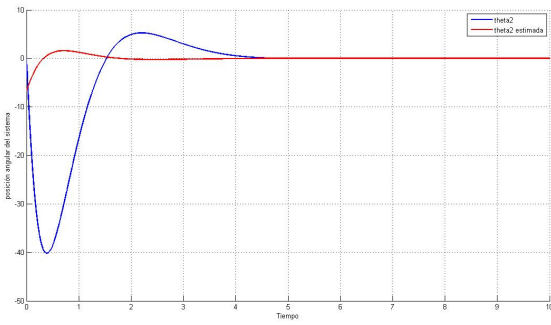


Figure 8.  $\theta_2$  and  $\hat{\theta}_2$

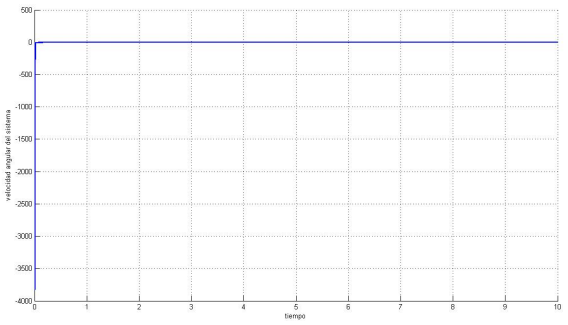


Figure 12. Closed loop system angular speed  $\theta_2$

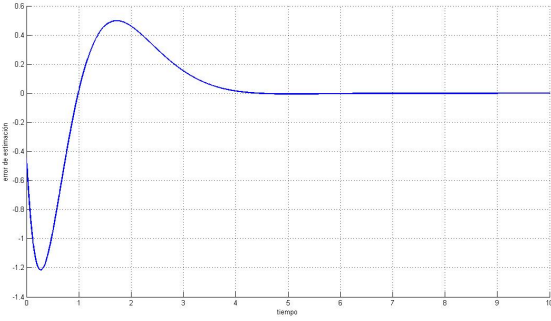


Figure 9. Closed loop system error

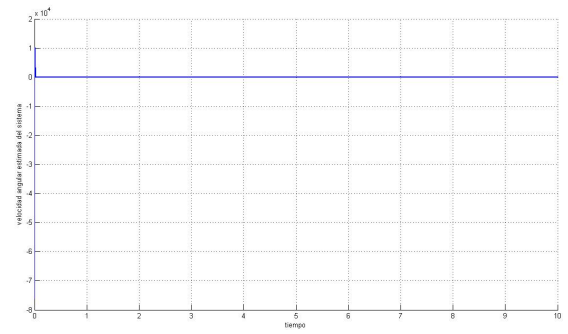


Figure 13. Closed loop system estimated angular velocity  $\hat{\theta}_2$

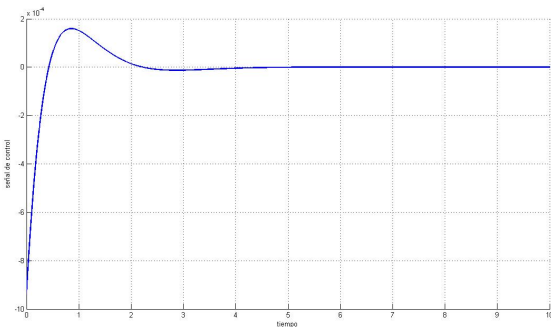


Figure 10. Closed loop system control signal

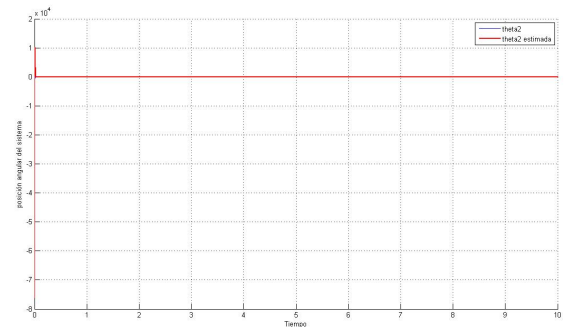


Figure 14.  $\theta_2$  and  $\hat{\theta}_2$

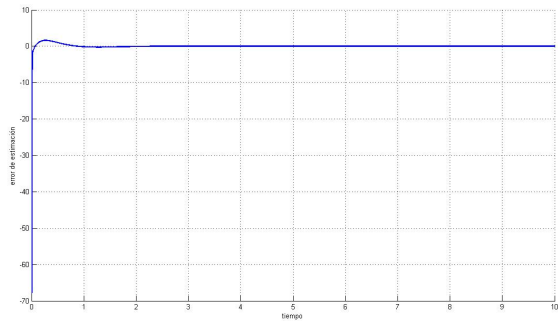


Figure 15. Closed loop system error

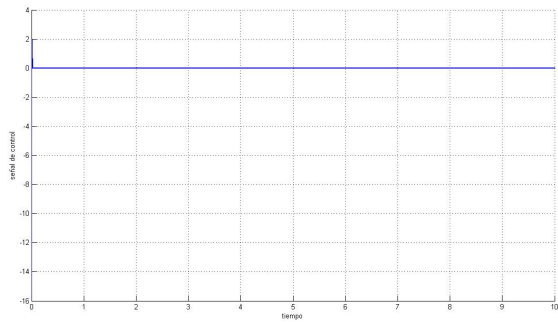


Figure 16. Closed loop system signal control

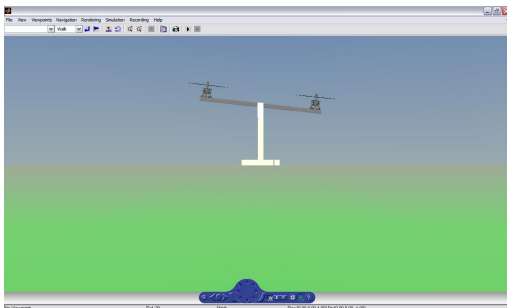


Figure 17. System stabilization

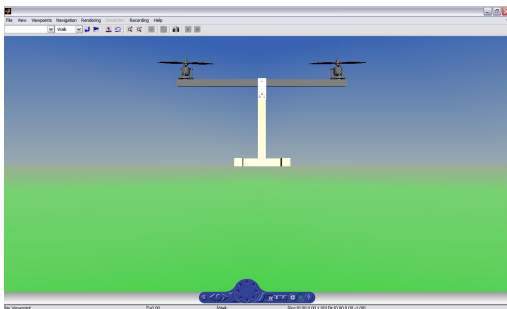


Figure 18. Stable system